

# Nonadiabatic dissociation of molecular condensates: competition between multi-mode reaction channels

Rajesh K. Malla<sup>1,\*</sup>

<sup>1</sup>*Center for Nonlinear Studies and Theoretical Division,  
Los Alamos National Laboratory, Los Alamos, New Mexico 87545, USA*

We formulate and solve a model describing a nonadiabatic dissociation process of molecular condensates. The dynamical process includes multi-mode reaction channels and the competition between channel parameters leads to a non-trivial dependence on key components such as path interference and symmetries. We find an analytical solution under *CPT* symmetry, where *C* is charge conjugation, *P* is parity, and *T* is time-reversal symmetry. Our solution predicts a population imbalance between atomic modes that is exponentially sensitive to channel parameters. A weakly broken symmetry, however, alters the population at each atomic mode and can reverse the population imbalance. Our solution also demonstrates strong quantum correlation between atomic modes that leads to spontaneous production of atoms in a multi-mode squeezed state. Moreover, our results are applicable in solving time-dependent *PT*-symmetric quantum mechanics which naturally manifests in the dissociation mechanism.

Motivated by a recent experiment [1], we previously solved an integrable model describing a coherent conversion mechanism between a molecular Bose-Einstein condensate (BEC) and an atomic BEC when their corresponding modes are swept through the Feshbach resonance [2]. Over the past two decades, there has been a tremendous surge in the theoretical [3–6] and experimental [7–11] studies on reaction between ultracold molecules and atoms near Feshbach resonance. However, in almost all cases the atomic modes are restricted to either a single mode or two modes where the dissociation process is controlled by a single parameter. This fails to capture various non-trivial effects such as interference, symmetry breaking, which may emerge due to competition between various modes corresponding to higher degrees of freedom, i.e. spin angular momentum, rotational and vibrational modes.

The general Hamiltonian describing reaction between atoms and molecules is given by

$$\begin{aligned} \hat{H} = & \sum_n \epsilon_n^\Psi \hat{\Psi}_n^\dagger \hat{\Psi}_n + \sum_{k,n} \epsilon_{k,n}^a \hat{a}_{k,n}^\dagger \hat{a}_{k,n} + \epsilon_{k,n}^b \hat{b}_{k,n}^\dagger \hat{b}_{k,n} \\ & + \sum_{k,n,m} g_{k,n,m} \hat{\Psi}_n^\dagger \hat{a}_{k,m} \hat{b}_{k,n-m} + g_{k,n,m}^* \hat{\Psi}_n \hat{a}_{k,m}^\dagger \hat{b}_{k,n-m}^\dagger, \end{aligned} \quad (1)$$

where  $k$  is the reaction channel [2],  $\hat{\psi}(\hat{\psi}^\dagger)$ ,  $\hat{a}(\hat{a}^\dagger)$ , and  $\hat{b}(\hat{b}^\dagger)$  represent annihilation (creation) of the molecular field operators and atomic field operators,  $n$  corresponding to a particular molecular mode. This mechanism can also describe cosmological production of particles and anti-particles due to vacuum fluctuations in the early stage of the Universe, which may have been a consequence of fundamental parameters such as mass or interaction coefficients becoming time-dependent and the evolution passing through resonance [12].

Hamiltonian (1) in general is not analytically solvable. We propose to solve this model in a mean-field approximation where the molecular operators are replaced by their expectation values [3]. For this approximation to hold, we assume that the number of atoms produced are small in comparison with the number of molecules. We choose to solve a model describing the dissociation mechanism of diatomic molecules into spin 1/2 atoms,  $AB \rightarrow A + B$ , where multiple atomic modes emerge when one considers the molecular condensates to be in three states, with  $S_z = 0, \pm 1$ , corresponding to singlet and triplets, respectively. The dissociated atoms can be either in spin-up state or spin-down state. The final population at each atomic mode is determined by the atomic field operators that satisfy a *non-Hermitian* Schrödinger equation, with anti-Hermitian coupling parameters.

There are two types of dissociation processes, stimulated dissociation and spontaneous dissociation. In the stimulated process an initially populated atomic mode (or modes) stimulates the dissociation of molecules. In the spontaneous process the atomic modes are initially empty and the molecules spontaneously dissociate into atoms.

In this paper, we predict several key results for our four-mode model. First, the analytical result predicts an exponential sensitive imbalance of atomic population in each mode. For example, an atomic mode initially occupied with an up-spin atom stimulates an exponentially suppressed atomic production in down-spin states. This suppression is an artifact of destructive interference which arises due to the *CPT* symmetry. A weakly broken symmetry, however, alters the atomic production in each mode and can reverse the spin imbalance for a finite interference. Our second key result appears in the spontaneous process, where the atomic modes are quantum correlated and the atoms are produced in a multi-mode squeezed state. Multi-mode squeezed states promise applications in quantum metrology [13], quantum communication, and quantum imaging [14–16]. In addition to these two central results, our solution for

\* malla@lanl.gov

a time-dependent PT-symmetric dynamics could open pathways for new investigations in time-dependent non-Hermitian systems.

We begin with a brief discussion on simple dissociation process of a molecular BEC into two-mode atomic condensate,  $AB \rightarrow A + B$ . The Hamiltonian (1) simplifies to [3, 17]

$$\hat{H}_2 = \mu_1(t)\hat{a}^\dagger\hat{a} + \mu_2(t)\hat{b}^\dagger\hat{b} + J\hat{\psi}^\dagger\hat{a}\hat{b} + J^*\hat{\psi}\hat{a}^\dagger\hat{b}^\dagger, \quad (2)$$

where  $\mu_i(t)$  are the time-dependent chemical potentials of atomic modes, and the chemical potential of molecular mode can be re-scaled to zero. In the nonadiabatic limit, only a small fraction of molecules get converted into atoms [4]. For large number of molecules we can assume the molecular condensate to be a reservoir and replace the molecular field operator with the expectation value  $\langle\hat{\psi}\rangle$ . The system then describes two interacting atomic modes and the effective Hamiltonian reads

$$\hat{H}_{eff}(t) = \mu_1(t)\hat{a}^\dagger\hat{a} + \mu_2(t)\hat{b}^\dagger\hat{b} + g\hat{a}\hat{b} + g^*\hat{a}^\dagger\hat{b}^\dagger. \quad (3)$$

The model (3) can be solved in the Heisenberg picture where the Schrödinger equation of atomic field operators  $\hat{a}(t)$  and  $\hat{b}(t)$  reads

$$i\frac{d}{dt}\begin{pmatrix} \hat{a}(t) \\ \hat{b}^\dagger(t) \end{pmatrix} = \begin{pmatrix} \mu_1(t) & g^* \\ -g & \mu_2(t) \end{pmatrix} \begin{pmatrix} \hat{a}(t) \\ \hat{b}^\dagger(t) \end{pmatrix}. \quad (4)$$

The molecular dissociation occurs near the crossing of two chemical potentials where the chemical potentials can be linearized.

The number of atoms in  $A$  mode at time  $t \rightarrow \infty$  is given by

$$\langle\hat{a}^\dagger(t)\hat{a}(t)\rangle_{t\rightarrow\infty} = n_{sp}^{(A)} + n_{st}^{(A)}, \quad (5)$$

where  $n_{sp}$  corresponds to spontaneous dissociation while  $n_{st}$  represents stimulated dissociation. For a linear sweep,  $\mu_1(t) = \beta t, \mu_2(t) = -\beta t$ , equation (4) resembles a non-Hermitian Landau-Zener (nLZ) model, and can be solved exactly, see Supplementary material (SM) [18]. The general solution of  $\hat{a}(t)$  has the form  $\hat{a}(t) = \phi_A(t)\hat{a}(t_0) + \phi_B(t)\hat{b}^\dagger(t_0)$ , where  $t_0$  represents the initial time and is assumed to be far away from the level crossing. The asymptotic solution of  $\phi_A(t \rightarrow \infty)$  and  $\phi_B(t \rightarrow \infty)$ , with initial condition  $\phi_A(t_0 \rightarrow -\infty) = 1, \phi_B(t_0 \rightarrow -\infty) = 0$ , leads to the expressions

$$|\phi_A(\infty)|^2 = |\phi_B(\infty)|^2 + 1 = \exp\left(\frac{\pi|g|^2}{\beta}\right). \quad (6)$$

In contrast to the Hermitian LZ model where  $|\phi_A(\infty)|^2 + |\phi_B(\infty)|^2 = 1$ , the non-Hermiticity conserves the difference  $|\phi_A(\infty)|^2 - |\phi_B(\infty)|^2 = 1$ .

The number of atoms in spontaneous dissociation is  $n_{sp}^{(A)} = |\phi_B(\infty)|^2$  [3, 17]. The spontaneous dissociation process is quantum correlated and the atoms are produced in a two-mode squeezed state, where the maximum uncertainty along one direction is exponentially suppressed with the exponent proportional to  $|g|^2/|\beta|$ .

The number of stimulated atoms in mode  $A$  depends on the initial population of  $A$  and  $B$  modes and the phases of the solutions  $\phi_A(t)$  and  $\phi_B(t)$  at large times [17]. If only the  $A$  mode is initially populated with a single atom, then the number of atoms in the  $A$  mode is  $|\phi_A(\infty)|^2$  and in the  $B$  mode is  $|\phi_B(\infty)|^2$ . Since the atoms are always produced in pairs the population difference between  $n_{st}^{(A)}$  and  $n_{st}^{(B)}$  is conserved, which agrees with equation (6).

*Multi-mode reaction channels.*— Now we focus on molecular dissociation in multi-mode reaction channels. We begin with an example of a dissociation process when molecules from three molecular modes, with spin angular momentum  $S_z = 0, \pm 1$ , dissociate into atoms with  $S_z = \pm 1/2$ . The dynamics of this complex mechanism can be captured by Hamiltonian (1). The time-dependence of chemical potentials of molecular modes can be re-scaled and absorbed into the time dependence of atomic modes, and the four-mode interacting system is now given by

$$\begin{aligned} \hat{H}_4 = & \mu_1(t)(\hat{a}_\uparrow^\dagger\hat{a}_\uparrow - \hat{a}_\downarrow^\dagger\hat{a}_\downarrow) + \mu_2(t)(\hat{b}_\uparrow^\dagger\hat{b}_\uparrow - \hat{b}_\downarrow^\dagger\hat{b}_\downarrow) \\ & + [J_1\hat{\psi}_{\uparrow\uparrow}^\dagger\hat{a}_\uparrow\hat{b}_\uparrow + J_1\hat{\psi}_{\downarrow\downarrow}^\dagger\hat{a}_\downarrow\hat{b}_\downarrow + J_2\hat{\psi}_{\uparrow\downarrow}^\dagger\hat{a}_\uparrow\hat{b}_\downarrow - J_2\hat{\psi}_{\downarrow\uparrow}^\dagger\hat{a}_\downarrow\hat{b}_\uparrow + h.c.], \end{aligned} \quad (7)$$

where the coupling parameters describing dissociation of triplet ( $S_z = \pm 1$ ) molecules are symmetric while the coupling parameters describing dissociation of singlet ( $S_z = 0$ ) molecules are anti-symmetric. This anti-symmetric nature emerges due to the spin-orbit coupling [19].

We solve (7) in the mean-field approximation and replace all the molecular operators with their expectation values. For a linear sweep, the Schrödinger equation of the atomic field operators is governed by a non-hermitian Hamiltonian. In the basis  $\hat{\Phi}(t) = \{\hat{a}_\uparrow(t), \hat{a}_\downarrow(t), \hat{b}_\uparrow^\dagger(t), \hat{b}_\downarrow^\dagger(t)\}$ , the Hamiltonian has the form

$$H_4^{(o)}(t) = \begin{pmatrix} b_1t + E_1 & 0 & g^* & -\gamma^* \\ 0 & -b_1t + E_1 & \gamma^* & g^* \\ -g & -\gamma & b_2t + E_2 & 0 \\ \gamma & -g & 0 & -b_2t + E_2 \end{pmatrix}, \quad (8)$$

where the coupling parameters are  $g = J_1\langle\hat{\psi}_{\uparrow\uparrow}\rangle$  and  $\gamma = J_2\langle\hat{\psi}_{\uparrow\downarrow}\rangle$ . The parameters  $b_1$  and  $b_2$  are the slopes of the chemical potentials and  $E_i$  correspond to level separations.

The non-Hermitian model (8) has a form similar to multi-state LZ (MLZ) model. The non-hermiticity leads to emergence complex eigen-energies near the crossing of diabatic (diagonal) level crossings. The anti-Hermitian couplings ensure that the eigen-energies near level crossing are complex conjugate of each other. This regime is known as PT-symmetry broken phase in the non-Hermitian literature. Note, in the two-mode level crossing there is one PT-broken phase [18, 20]. The model (8) however has four PT broken phases. In addition, the dynamics includes two paths, purple and green colors in

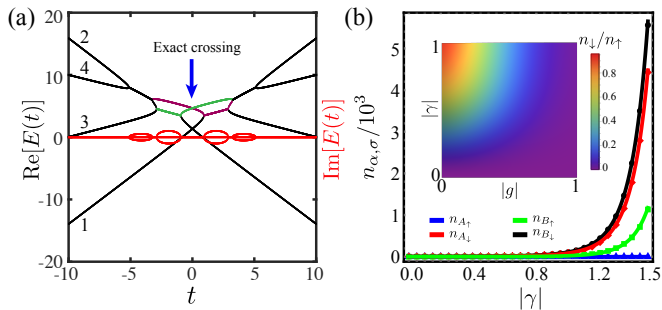


FIG. 1. (a) The instantaneous eigen-energies of (8) are shown as a function of time for parameters  $\beta_1 = -1, \beta_2 = 0.5, E_1 = 5, E_2 = 1, g = 0.5, \gamma = 1$ . The black curves are real energies and the red curves represent imaginary energies. (b) The number of atoms produced in a particular mode when the system was stimulated by a single atom in  $A_{\uparrow}$  mode. The scattered points are obtained from numerical evolution of (8) while the solid curves are obtained from the analytical formula in (12).

Fig. 1a, that can amount to a finite path interference in the system. The interplay between the PT broken phase and the path interference strongly affects the final occupation of the atomic modes at large times.

The solution of the Schrödinger equation for  $H_4^{(o)}(t)$  requires finding the matrix  $S$ , which satisfies  $|\hat{\Phi}(t \rightarrow -\infty)\rangle = S|\hat{\Phi}(t \rightarrow +\infty)\rangle$ , where  $S \equiv U(T, -T)_{T \rightarrow \infty}$  is a non-unitary matrix. In Hermitian dynamics  $S$  is commonly known as the scattering matrix. The number of atoms in each mode depends on the matrix elements  $S_{ij}$ . These elements, however, cannot be obtained analytically for any arbitrary complex parameters  $g$  and  $\gamma$  [21–23].

To find an analytically solvable model, We recall the recent development on integrability and solvability in various Hermitian MLZ models [24, 25]. The solvability conditions help us to find parameters for which the matrix  $S$  corresponding to (8) can be found analytically. The integrability allows us to extend the model to find a class of non-Hermitian models which commutes with (8). The solvability condition in the Hermitian dynamics reads [25]: (i) the transition probability which is equivalent to  $|S_{ij}|^2$  is independent of level spacing parameters  $E$  and (ii) the exact crossing of eigen-energies at intersections of diabatic states (i.e., diagonal elements of the Hamiltonian) without direct couplings.

In Ref. [25] it was also shown that the  $CPT$  symmetry is partially responsible for the solvability of the Hamiltonian. The  $CPT$  symmetry leads to the following relation between the elements of the  $S$  matrix:

$$\hat{S} = \hat{S}' \equiv \hat{C}\hat{P}\hat{T}\hat{S} = \begin{pmatrix} S_{22} & -S_{12} & S_{42} & -S_{32} \\ -S_{21} & S_{11} & -S_{41} & S_{31} \\ S_{24} & -S_{14} & S_{44} & -S_{34} \\ -S_{23} & S_{13} & -S_{43} & S_{33} \end{pmatrix} \quad (9)$$

where  $S_{ij}$  are the matrix elements of  $\hat{S}$  and the levels  $\{1, 2, 3, 4\}$  refer to the operators  $\{\hat{a}_{\uparrow}, \hat{a}_{\downarrow}, \hat{b}_{\uparrow}, \hat{b}_{\downarrow}\}$ , respec-

tively. From (9) we obtain the following relations:

$$S_{11} = S_{22}, S_{33} = S_{44}, S_{12} = S_{21} = S_{34} = S_{43} = 0. \quad (10)$$

The amplitude of the  $S$  matrix elements  $S_{ii}$ ,  $S_{13}$ , and  $S_{24}$  can be obtained in the independent crossing approximation [26]. The matrix elements  $S_{14}$  and  $S_{23}$  can be obtained under solvability, when one can substitute the level spacing parameters  $E_i$  to be zero, and the model (8) is equivalent to models with four modes crossing at a single point [27].

In the stimulated process, the number of atoms in each mode  $i$ , assuming that only level  $j$  is initially occupied, is given by  $n_{ij} = |S_{ij}|^2 n_{0j}$ , where  $n_{0j}$  is the number of atoms in the  $j$  mode at  $t \rightarrow \infty$ . Since, the atoms are always produced in pairs, the population difference between  $A$  and  $B$  is conserved and we obtain the following conservation of population difference

$$n_{11} - n_{31} - n_{41} = n_{01}. \quad (11)$$

Similar conservation conditions can be obtained for different initial conditions.

We find that our model (8) is solvable, when the phase difference between  $g$  and  $\gamma$  is  $\theta = n\pi$ , the dynamics of (8) is protected by  $CPT$  symmetry [18] and the  $S$  matrix has the form of (9). Note, the non-Hermiticity does not affect the form of the scattering matrix. Thus we obtain a matrix  $\hat{n}$  describing all possible  $n_{ij}$ :

$$\frac{\hat{n}}{n_0} = \begin{pmatrix} \tilde{n}_g \tilde{n}_{\gamma} & 0 & \tilde{n}_{\gamma}(\tilde{n}_g - 1) & \tilde{n}_{\gamma} - 1 \\ 0 & \tilde{n}_g \tilde{n}_{\gamma} & \tilde{n}_{\gamma} - 1 & \tilde{n}_{\gamma}(\tilde{n}_g - 1) \\ \tilde{n}_{\gamma}(\tilde{n}_g - 1) & \tilde{n}_{\gamma} - 1 & \tilde{n}_g \tilde{n}_{\gamma} & 0 \\ \tilde{n}_{\gamma} - 1 & \tilde{n}_{\gamma}(\tilde{n}_g - 1) & 0 & \tilde{n}_g \tilde{n}_{\gamma} \end{pmatrix}, \quad (12)$$

where  $n_0 = n_{0i}$  is the number of initial atoms in a particular mode,  $\tilde{n}_g = e^{\frac{\pi|g|^2}{2|\beta_2|}}$ ,  $\tilde{n}_{\gamma} = e^{\frac{\pi|\gamma|^2}{2|\beta_1|}}$ ,  $2\beta_1 = b_1 + b_2$ , and  $2\beta_2 = b_1 - b_2$ . Here,  $\tilde{n}_g$  and  $\tilde{n}_{\gamma}$  correspond to the non-Hermitian LZ transitions at diabatic level crossings [18].

The number of stimulated atoms in each mode is shown in Fig. 1b, when  $A_{\uparrow}$  is initially populated with a single atom. We find that our analytical prediction (12) perfectly agrees with the results obtained from numerical simulation of the Schrödinger equation. The number of atoms in  $A_{\downarrow}$  mode is zero, as predicted by the  $CPT$  symmetry. This is an artifact of destructive interference due to complete cancellation of two competing reaction channels as shown in Fig. 1a. The total number of down spins is purely produced in the  $B_{\downarrow}$  mode. The ratio between total number of down spin atoms and total number of up spin atoms is then given by the formula

$$\frac{n_{\downarrow}}{n_{\uparrow}} = \frac{\tilde{n}_{\gamma} - 1}{2\tilde{n}_g \tilde{n}_{\gamma} - \tilde{n}_{\gamma}}. \quad (13)$$

For a small value of  $|\gamma|^2/\beta_1$ , the expression can be reduced to  $n_{\downarrow}/n_{\uparrow} = e^{-\frac{\pi|g|^2}{2|\beta_2|}} (|\gamma|^2/2|\beta_1|)$ , which is exponentially suppressed with parameter  $|g|^2/|\beta_2|$  and depends

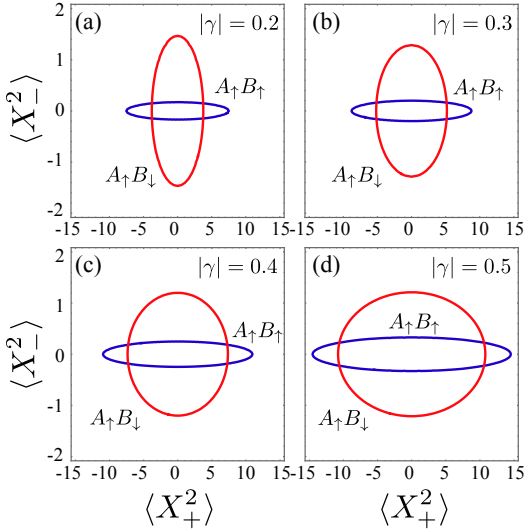


FIG. 2. The pairwise squeezing of  $A$  and  $B$  modes is shown from (15) and (16) and the constant shift is ignored in both directions. The parameters are  $|g| = 0.5$  and  $|\beta_1| = |\beta_2| = 1$ .

linearly on parameter  $|\gamma|^2/|\beta_1|$ . This peculiar dependence is shown in the parametric plot in the inset of Fig. 1b.

*Emergence of multi-mode squeezed states due to spontaneous emission.*— The spontaneous dissociation process in the four-mode model (8) is quantum correlated. The number of atoms in each mode can be obtained from (12) and is given by

$$n_{\alpha,\sigma} = \tilde{n}_g \tilde{n}_\gamma - 1, \quad (14)$$

where  $\alpha$  refers to  $A$  or  $B$  and  $\sigma$  refers to the spin orientation. The solvability of our model allows us to evaluate pair-wise squeezing of atomic modes. First, we observe that the modes  $A_\uparrow$  and  $A_\downarrow$  are not quantum correlated and are not in a two-mode squeezed state. The maximum uncertainty along both  $X_+$  and  $X_-$  is equal, where  $X$  is the position operator of two-mode squeezed state. The same applies to modes  $B_\uparrow$  and  $B_\downarrow$ .

Therefore, the atoms produced in the spontaneous process are always in a three-mode squeezed state [28]. To observe squeezing between  $A_\uparrow$  and  $B_\uparrow$  ( $B_\downarrow$ ), we evaluate  $\langle X_\pm^2 \rangle$  and find the maximum values along each direction  $X_\pm$  is given by

$$\langle X_\pm^2 \rangle_{A_\uparrow B_\uparrow} = c_\gamma + \frac{1}{2} |(\tilde{n}_g \tilde{n}_\gamma)^{1/2} \pm ((\tilde{n}_g - 1) \tilde{n}_\gamma)^{1/2}|^2, \quad (15)$$

$$\langle X_\pm^2 \rangle_{A_\uparrow B_\downarrow} = c_{g\gamma} + \frac{1}{2} |(\tilde{n}_g \tilde{n}_\gamma)^{1/2} \pm (\tilde{n}_\gamma - 1)^{1/2}|^2, \quad (16)$$

where  $c_\gamma = \frac{\tilde{n}_\gamma - 1}{2}$  and  $c_{g\gamma} = \frac{\tilde{n}_\gamma \tilde{n}_g - 1}{2}$  are constant shifts. In Fig. 2 we plot  $\langle X_\pm^2 \rangle$  for different values of  $|\gamma|$ . The atoms produced in  $A_\uparrow$  and  $B_\uparrow$  mode are always squeezed along the  $X_-$  direction and this phenomenon has the same origin as squeezing in a simple two-mode atomic dissociation. The atoms in  $A_\uparrow$  and  $B_\downarrow$  modes are squeezed

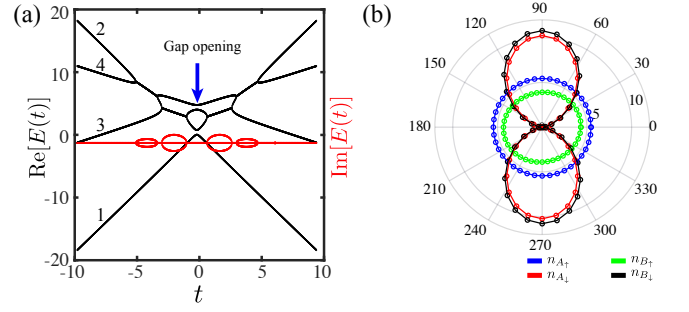


FIG. 3. (a) The instantaneous eigen-energies of (8) are shown as a function of time for parameters  $\beta_1 = -1, \beta_2 = 0.5, E_1 = 5, E_2 = 1, g = 0.5, \gamma = i$ . The black curves are real energies and the red curves represent imaginary energies. (b) The stimulated population of atomic modes from initially prepared single atom in  $A_\uparrow$  is shown as a function of  $\theta$ . The colors blue, green, red, and black correspond to atomic modes  $A_\uparrow, B_\uparrow, A_\downarrow,$  and  $B_\downarrow$ , respectively.

along  $X_+$  for small values of  $|\gamma|$ . This squeezing is suppressed with increase in  $|\gamma|$ , and eventually changes to  $X_-$  direction. From the symmetry of couplings we find that the squeezing for up-spin  $A$  and  $B$  modes and down-spin  $A$  and  $B$  modes is equal, while the squeezing between up-spin  $A$  and down-spin  $B$  modes is the same as down-spin  $A$  and up-spin  $B$  modes.

*Phase difference between  $g$  and  $\gamma$  and broken solvability.*— Now we discuss the scenario when there is a finite phase difference between  $g$  and  $\gamma$ . This finite phase difference,  $\theta$ , is responsible for violation of  $CPT$  symmetry and gaps emerge near the exact crossing of levels with opposite slopes, see Fig. 3a. This violation of exact crossing leads to asymmetric phase accumulations along the two interfering paths which leads to a finite interference in the system. Due to the finite interference, initial atoms in  $A_\uparrow$  mode can stimulate the production of atoms in  $A_\downarrow$  mode. An exact analytical solution, however, is not possible and we turn to numerical approach.

In Fig. 3b, we show the  $\theta$  dependence of number of atoms in each mode stimulated by a single atom in  $A_\uparrow$  mode. For  $\theta = 0$  or  $\pi$  we recover the solvability condition and the  $CPT$  symmetry of the Schrödinger equation, which indeed agree with formula (13), and the down-spin atoms are exponentially suppressed. The production of down-spin atoms increases with increasing  $\theta$ , which corresponds to widening of the gaps and stronger constructive interference, see Fig. 3b. Note, the imaginary parts of the eigen-energies, however, remain unaffected. At  $\theta = (2m + 1)\pi/2$ , the interference becomes constructive and a maximum down spin production is stimulated.

Concerning spontaneous dissociation, the total number atoms in each mode is no longer equal, however they still satisfy the condition  $n_{A_\uparrow} + n_{A_\downarrow} = n_{B_\uparrow} + n_{B_\downarrow}$ . The condition that atoms are produced in pairs ensures the quantum correlation between modes and here the atoms will be produced in four-mode squeezing due to an effective coupling between  $A_\uparrow$  and  $A_\downarrow$ .

In Conclusion, we have solved a mechanism of dissociation of molecular condensate when there are competing multi-mode channels. In comparison to prior studies, our model can be used to distinguish between the types of atoms produced, and the parameters can be tailored to find an on-demand mixture of different types of atoms. The multi-mode squeezed atoms can be used for multi-channel quantum applications which will add additional degrees of freedom to quantum communication. Our article also sheds light on solving a linearly time-dependent non-Hermitian dynamics that includes PT broken phases.

## ACKNOWLEDGEMENTS

I thank Nikolai Sinitsyn, Avadh Saxena, Julia Cen, Mikhail Raikh, Wilton Kort-Kamp, and Saikat Banerjee for useful discussions. This work was supported by the U.S. Department of Energy, Office of Science, Basic Energy Sciences, Materials Sciences and Engineering Division, Condensed Matter Theory Program, and the LANL Center for Nonlinear Studies.

- 
- [1] Zhendong Zhang, Liangchao Chen, Kai-Xuan Yao, and Cheng Chin, “Transition from an atomic to a molecular Bose-Einstein condensate,” *Nature* **592**, 708–711 (2021).
- [2] Rajesh K. Malla, Vladimir Y. Chernyak, Chen Sun, and Nikolai A. Sinitsyn, “Coherent reaction between molecular and atomic bose-einstein condensates: integrable model,” (2022), [arXiv:2112.12302 \[quant-ph\]](https://arxiv.org/abs/2112.12302).
- [3] V. A. Yurovsky, A. Ben-Reuven, and P. S. Julienne, “Quantum effects on curve crossing in a Bose-Einstein condensate,” *Phys. Rev. A* **65**, 043607 (2002).
- [4] Alexander Altland, V. Gurarie, T. Kriecherbauer, and A. Polkovnikov, “Nonadiabaticity and large fluctuations in a many-particle Landau-Zener problem,” *Phys. Rev. A* **79**, 042703 (2009).
- [5] Chen Sun and Nikolai A. Sinitsyn, “Landau-Zener extension of the Tavis-Cummings model: Structure of the solution,” *Phys. Rev. A* **94**, 033808 (2016).
- [6] A. P. Itin and P. Törmä, “Dynamics of a many-particle Landau-Zener model: Inverse sweep,” *Phys. Rev. A* **79**, 055602 (2009).
- [7] Jens Herbig, Tobias Kraemer, Michael Mark, Tino Weber, Cheng Chin, Hanns-Christoph Nägerl, and Rudolf Grimm, “Preparation of a pure molecular quantum gas,” *Science* **301**, 1510–1513 (2003).
- [8] K. Xu, T. Mukaiyama, J. R. Abo-Shaer, J. K. Chin, D. E. Miller, and W. Ketterle, “Formation of quantum-degenerate sodium molecules,” *Phys. Rev. Lett.* **91**, 210402 (2003).
- [9] John L. Bohn, Ana Maria Rey, and Jun Ye, “Cold molecules: Progress in quantum engineering of chemistry and quantum matter,” *Science* **357**, 1002–1010 (2017).
- [10] S. Matyjaśkiewicz, M. H. Szymańska, and K. Góral, “Probing fermionic condensates by fast-sweep projection onto Feshbach molecules,” *Phys. Rev. Lett.* **101**, 150410 (2008).
- [11] M. Duda, X-Y. Chen, A. Schindewolf, R. Bause, J. Milczewski, I. Schmidt, R. Bloch, and X-Y. Luo, “Transition from a polaronic condensate to a degenerate Fermi gas of heteronuclear molecules,” Preprint [arXiv:2111.04301](https://arxiv.org/abs/2111.04301) (2021).
- [12] Daniel Green and Rafael A. Porto, “Signals of a quantum universe,” *Phys. Rev. Lett.* **124**, 251302 (2020).
- [13] Manuel Gessner, Luca Pezzè, and Augusto Smerzi, “Sensitivity bounds for multiparameter quantum metrology,” *Phys. Rev. Lett.* **121**, 130503 (2018).
- [14] A. S. Coelho, F. A. S. Barbosa, K. N. Cassemiro, A. S. Villar, M. Martinelli, and P. Nussenzveig, “Three-color entanglement,” *Science* **326**, 823–826 (2009), <https://www.science.org/doi/pdf/10.1126/science.1178683>.
- [15] Christoph Simon, Hugues de Riedmatten, Mikael Afzelius, Nicolas Sangouard, Hugo Zbinden, and Nicolas Gisin, “Quantum repeaters with photon pair sources and multimode memories,” *Phys. Rev. Lett.* **98**, 190503 (2007).
- [16] L. M. Duan, M. D. Lukin, J. I. Cirac, and P. Zoller, “Long-distance quantum communication with atomic ensembles and linear optics,” *Nature* **414**, 413–418 (2001).
- [17] M. A. Kayali and N. A. Sinitsyn, “Formation of a two-component Bose condensate during the chemical-potential curve crossing,” *Phys. Rev. A* **67**, 045603 (2003).
- [18] “Supplementary material, which additionally cites refs. [29, 30], has three sections with (i) comments on non-hermitian landau-zener model; (ii) exact solution of our solvable model; and (iii) derivation of pairwise squeezing.”
- [19] Y. J. Lin, K. Jiménez-García, and I. B. Spielman, “Spin-orbit-coupled bose-einstein condensates,” *Nature* **471**, 83–86 (2011).
- [20] B. Longstaff and E.-M. Graefe, “Nonadiabatic transitions through exceptional points in the band structure of a pt-symmetric lattice,” *Phys. Rev. A* **100**, 052119 (2019).
- [21] Rajesh K. Malla and M. E. Raikh, “Loss of adiabaticity with increasing tunneling gap in nonintegrable multistate landau-zener models,” *Phys. Rev. B* **96**, 115437 (2017).
- [22] Rajesh K. Malla, Vladimir Y. Chernyak, and Nikolai A. Sinitsyn, “Nonadiabatic transitions in landau-zener grids: Integrability and semiclassical theory,” *Phys. Rev. B* **103**, 144301 (2021).
- [23] Bin Yan, Vladimir Y. Chernyak, Wojciech H. Zurek, and Nikolai A. Sinitsyn, “Nonadiabatic phase transition with broken chiral symmetry,” *Phys. Rev. Lett.* **126**, 070602 (2021).
- [24] Nikolai A. Sinitsyn, Emil A. Yuzbashyan, Vladimir Y. Chernyak, Aniket Patra, and Chen Sun, “Integrable time-dependent quantum hamiltonians,” *Phys. Rev. Lett.* **120**, 190402 (2018).
- [25] N. A. Sinitsyn, “Solvable four-state landau-zener model of two interacting qubits with path interference,” *Phys. Rev. B* **92**, 205431 (2015).
- [26] Yu. N. Demkov and V. N. Ostrovsky, “Multipath interference in a multistate landau-zener-type model,” *Phys. Rev. A* **61**, 032705 (2000).

- [27] Fuxiang Li, Chen Sun, Vladimir Y. Chernyak, and Nikolai A. Sinitsyn, “Multistate landau-zener models with all levels crossing at one point,” *Phys. Rev. A* **96**, 022107 (2017).
- [28] S. Rojas-Rojas, E. Barriga, C. Muñoz, P. Solano, and C. Hermann-Avigliano, “Manipulation of multimode squeezing in a coupled waveguide array,” *Phys. Rev. A* **100**, 023841 (2019).
- [29] “Higher transcendental functions, edited by a. erdelyi, vol. 2 (mcgraw-hill, new york, 1953).” .
- [30] Rajesh K. Malla, E. G. Mishchenko, and M. E. Raikh, “Suppression of the landau-zener transition probability by weak classical noise,” *Phys. Rev. B* **96**, 075419 (2017).

Supplementary Material: “Nonadiabatic dissociation of molecular condensates:  
competition between multi-mode reaction channels”

Rajesh K. Malla<sup>1,\*</sup>

<sup>1</sup>*Center for Nonlinear Studies and Theoretical Division,  
Los Alamos National Laboratory, Los Alamos, New Mexico 87545, USA*

arXiv:2202.08468v1 [quant-ph] 17 Feb 2022

---

\* [malla@lanl.gov](mailto:malla@lanl.gov)

## I. NON-HERMITIAN LANDAU-ZENER MODEL

The non-Hermitian Landau-Zener (nLZ) model can be described by the Hamiltonian

$$\hat{H}_{nLZ} = \begin{pmatrix} \beta t & g \\ -g^* & -\beta t \end{pmatrix}, \quad (1)$$

where  $\pm\beta$  are the two slopes corresponding to two levels and  $g$  is the level coupling, which in general is complex. Unlike the Hermitian model the level couplings  $g$  and  $-g^*$  are negative complex conjugate of each other. The eigen-energies of  $\hat{H}_{nLZ}$  are given by

$$E_{nLZ}(t) = \pm\sqrt{\beta^2 t^2 - |g|^2}. \quad (2)$$

In standard LZ model the eigen-energies are given by  $E_{LZ} = \pm\sqrt{\beta^2 t^2 + |g|^2}$ . The eigen-energies  $E_{nLZ}(t)$  are shown

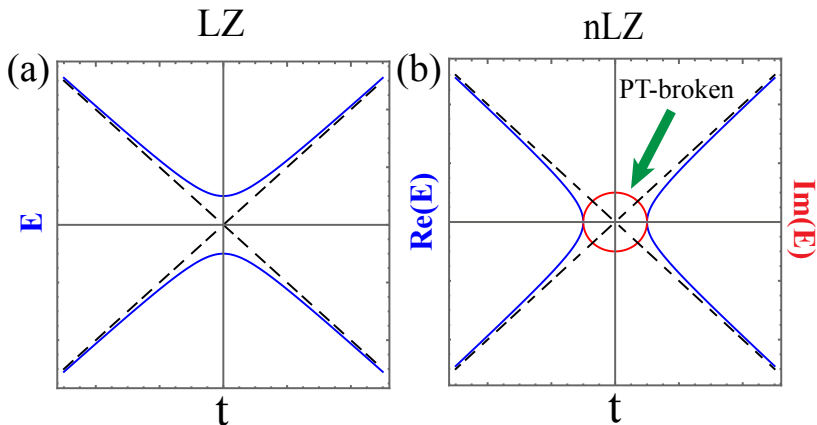


FIG. 1. The eigen-energies of (a) standard LZ model and (b) the nLZ model ( $E_{nLZ}(t)$ ) are schematically shown as a function of time. The blue corresponds to real part of eigen energy while the red corresponds to the imaginary part.

as a function of time in Fig. 1b together with the eigen-energies for a standard LZ model with parameter  $\beta$  and  $g$ .

The solution of the Schrödinger equation for Hamiltonian (1) has the form of a  $2 \times 1$  column vector,

$$|\phi(t)\rangle = \begin{pmatrix} a(t) \\ b(t) \end{pmatrix},$$

where  $a(t)$  satisfies a second order differential equation

$$\ddot{a}(t) + (\beta^2 t^2 - |g|^2 + i\beta)a(t) = 0, \quad (3)$$

whose solutions are given by parabolic cylinder functions [1].

The solution can now be expressed as follows [2]

$$|\phi(t)\rangle = \begin{pmatrix} a(t) \\ b(t) \end{pmatrix} = \phi_1 \begin{pmatrix} D_\nu(z) \\ -i\sqrt{\nu}D_{\nu-1}(z) \end{pmatrix} + \phi_2 \begin{pmatrix} D_\nu(-z) \\ -i\sqrt{\nu}D_{\nu-1}(-z) \end{pmatrix}, \quad (4)$$

where  $D_\nu(z)$  is the parabolic cylinder function, with  $\nu = i|g|^2/2\beta$  and  $z = \sqrt{2\beta}e^{i\pi/4}t$ . Since we are only interested in the dynamics at large times  $t \rightarrow \pm\infty$ , the asymptotic behavior of parabolic cylinder functions is good enough for our analysis. The key difference between the Hermitian and non-Hermitian dynamics comes from the phase of  $\nu$ , which is  $-\pi/2$  for the Hermitian case and  $\pi/2$  for the non-Hermitian case. This crucial difference leads to the following difference between LZ and nLZ dynamics. Assuming the system starts with the upper state,  $|a(t \rightarrow -\infty)|^2 = 1$ , the asymptotic solution of  $a(t)$  at large positive times is given by  $|a(t \rightarrow \infty)|^2 = e^{-\pi|g|^2/\beta}$  for the Hermitian model and  $|a(t \rightarrow \infty)|^2 = e^{\pi|g|^2/\beta}$  for the non-Hermitian model. Similarly, the solution  $b(t)$  at large positive times is given by  $|b(t \rightarrow \infty)|^2 = 1 - e^{-\pi|g|^2/\beta}$  for the Hermitian model and  $|b(t \rightarrow \infty)|^2 = e^{\pi|g|^2/\beta} - 1$  for the non-Hermitian model.

This exponential dependence in the non-Hermitian model appears due to the anti-Hermitian complex couplings. The conservation law in the Hermitian model describes the standard probability law

$$|a(t)|^2 + |b(t)|^2 = 1.$$

The probability of survival is given by  $|a(t \rightarrow \infty)|^2$  while the probability of adiabatic transition is given by  $|b(t \rightarrow \infty)|^2$ . In the non-Hermitian model, however, there are no such terms and the exponentially growing nature makes it difficult to call it probability. Nevertheless, in our model,  $|a(t \rightarrow \infty)|^2$  and  $|b(t \rightarrow \infty)|^2$  correspond to the number of atoms produced in the respective atomic modes. The conservation law here results from the asymptotic expansion of parabolic cylinder functions,

$$|a(t)|^2 - |b(t)|^2 = 1,$$

and agrees with our dissociation mechanism in which atoms are produced in pairs.

## II. EXACT SOLUTION FOR THE SOLVABLE MODEL

To check the CPT symmetry we write down the Schrödinger equation for our model (8) in the main text:

$$i \frac{d}{dt} \begin{pmatrix} \hat{a}_\uparrow \\ \hat{a}_\downarrow \\ \hat{b}_\uparrow \\ \hat{b}_\downarrow \end{pmatrix} = \begin{pmatrix} b_1 t + E_1 & 0 & g^* & -\gamma^* \\ 0 & -b_1 t + E_1 & \gamma^* & g^* \\ -g & -\gamma & b_2 t + E_2 & 0 \\ \gamma & -g & 0 & -b_2 t + E_2 \end{pmatrix} \begin{pmatrix} \hat{a}_\uparrow \\ \hat{a}_\downarrow \\ \hat{b}_\uparrow \\ \hat{b}_\downarrow \end{pmatrix}. \quad (5)$$

Equation (5) must remain invariant under three simultaneous operations:

- i.* time-reversal ( $\hat{T}$ ): change  $t \rightarrow -t$ ,  $\hat{a} \rightarrow \hat{a}^\dagger$ , and  $\hat{b}^\dagger \rightarrow \hat{b}$ ;
- ii.* complex conjugation ( $\hat{C}$ ): change the imaginary number  $i \rightarrow -i$ ,  $\hat{a} \rightarrow \hat{a}^\dagger$ , and  $\hat{b}^\dagger \rightarrow \hat{b}$ ;
- iii.* parity ( $\hat{P}$ ): rename amplitudes  $\hat{a}_\uparrow \rightarrow -\hat{a}_\downarrow$ ,  $\hat{a}_\downarrow \rightarrow \hat{a}_\uparrow$ ,  $\hat{b}_\uparrow \rightarrow -\hat{b}_\downarrow$ , and  $\hat{b}_\downarrow \rightarrow \hat{b}_\uparrow$ .

Now, it is straightforward to see that under the  $CPT$  operation, equation (5) remains invariant only when the phase difference between  $g$  and  $\gamma$  is  $n\pi$ .

Let us consider the  $S$  matrix for our 4-level problem corresponding to the non-Hermitian Hamiltonian  $H_4^{(o)}(t)$ . The  $S$  matrix refers to the matrix

$$S \equiv U(T, -T)_{T \rightarrow \infty}, \quad (6)$$

which is non-unitary. The non-unitarity comes from the complex energies near the diabatic level crossings and plays no role in determining the solvability of our model.

Our model has similarity with a particular subclass of Hermitian multi-state Landau-Zener (MLZ) problems, and the properties of scattering matrices for the Hermitian model are listed in Ref. [3], where the parameters  $g$  and  $\gamma$  are considered real. In the Hermitian model the transition probability is defined as  $P_{ij} = |S_{ij}|^2$ , and the probabilities satisfy the conservation of probability law, e.g.,  $\sum_j P_{ij} = 1$ . Here,  $P_{ij}$  refers to the transition probability to find an electron in the  $i$ -th state at large times  $t \rightarrow \infty$  starting from  $j$ -th state at initial time  $t \rightarrow -\infty$ . The exact solution refers to the analytical formula equation (15) in Ref. [3] for all the transition matrix elements.

In our non-Hermitian case, the coupling parameters  $g$  and  $\gamma$  satisfy the anti-Hermiticity condition. We argue that the complex gap opening near the level crossing only affects the amplitudes of the scattering matrix elements while the phases are still determined by real part of the eigen-energies. Therefore, the form of the scattering matrix must resemble with its Hermitian counterpart. Instead of transition probability, we define  $n_{ij} = |S_{ij}|^2$ , where  $n_{ij}$  refers to the number of atoms produced in the  $i$ -th mode when the  $j$ -th mode is initially populated with a single atom.

As discussed in the previous section, the dynamics near each PT-broken phase in a non-Hermitian multi-state Landau-Zener (nMLZ) model can be considered as an individual nLZ transition. Therefore, our result has similarity with equation (15) of Ref. [3]. However, we replace  $p_1$  with  $\tilde{n}_g$ ,  $p_2$  with  $\tilde{n}_\gamma$ ,  $q_1 = 1 - p_1$  with  $\tilde{n}_g - 1$ , and  $q_2 = 1 - p_2$  with  $\tilde{n}_\gamma - 1$ . After making these substitutions we arrive at our exact result equation (16) in the main text. The formula obeys the conservation law of pair production,

$$n_{jj} - \sum_i n_{ij} = n_j^{(0)} = 1, \quad (7)$$

where  $n_j^{(0)}$  corresponds to the the initial population (single atom) in the  $j$ -th mode.

### III. PAIRWISE SQUEEZING OF ATOMIC MODES

The spontaneous dissociation process is quantum correlated and the atoms are produced in multi-mode quantum squeezed states. To quantify squeezing, we define position operators for the two modes corresponding to different types atoms  $A$  and  $B$ . The position operator reads

$$\hat{X}_{A_\sigma B_{\sigma'}}^{(\phi)} = \frac{1}{2} \left[ e^{-i\phi} (\hat{a}_\sigma + \hat{b}_{\sigma'}) + e^{i\phi} (\hat{a}_\sigma^\dagger + \hat{b}_{\sigma'}^\dagger) \right], \quad (8)$$

where  $\sigma, \sigma'$  refer to the spins while  $\phi$  is the angle that defines the measured quadrature. It is straightforward to see that the expectation value of operator  $X$  is zero, while the expectation value of  $X^2$  can be non-zero. We expand the expression for the  $X^2$  operator from (8)

$$\hat{X}_{\pm, A_\sigma B_{\sigma'}}^{(\theta)^2} = \frac{1}{4} \left[ e^{-2i\phi} (\hat{a}_\sigma^2 + \hat{b}_{\sigma'}^2 + \hat{a}_\sigma \hat{b}_{\sigma'} + \hat{b}_{\sigma'} \hat{a}_\sigma) + \hat{a}_\sigma^\dagger \hat{a}_\sigma + \hat{a}_\sigma^\dagger \hat{b}_{\sigma'} + \hat{b}_{\sigma'}^\dagger \hat{a}_\sigma + \hat{b}_{\sigma'}^\dagger \hat{b}_{\sigma'} \right] + h.c. \quad (9)$$

At large times  $t \rightarrow \infty$ , the operators satisfy

$$\begin{aligned} \hat{a}_\uparrow(t) &= S_{11} \hat{a}_\uparrow(t_0) + S_{12} \hat{a}_\downarrow(t_0) + S_{13} \hat{b}_\uparrow^\dagger(t_0) + S_{14} \hat{b}_\downarrow^\dagger(t_0), \\ \hat{a}_\downarrow(t) &= S_{21} \hat{a}_\uparrow(t_0) + S_{22} \hat{a}_\downarrow(t_0) + S_{23} \hat{b}_\uparrow^\dagger(t_0) + S_{24} \hat{b}_\downarrow^\dagger(t_0), \\ \hat{b}_\uparrow^\dagger(t) &= S_{31} \hat{a}_\uparrow(t_0) + S_{32} \hat{a}_\downarrow(t_0) + S_{33} \hat{b}_\uparrow^\dagger(t_0) + S_{34} \hat{b}_\downarrow^\dagger(t_0), \\ \hat{b}_\downarrow^\dagger(t) &= S_{41} \hat{a}_\uparrow(t_0) + S_{42} \hat{a}_\downarrow(t_0) + S_{43} \hat{b}_\uparrow^\dagger(t_0) + S_{44} \hat{b}_\downarrow^\dagger(t_0). \end{aligned} \quad (10)$$

Here,  $t_0$  corresponds to initial time. The non-zero contribution to  $\langle X^2 \rangle$  comes from terms proportional to  $\langle \hat{a}(t_0) \hat{a}^\dagger(t_0) \rangle$  and  $\langle \hat{b}(t_0) \hat{b}^\dagger(t_0) \rangle$ . The term  $\langle \hat{a}(t_0) \hat{a}^\dagger(t_0) \rangle = 1 + \langle \hat{a}^\dagger(t_0) \hat{a}(t_0) \rangle$  and the second term vanishes since the initial atomic population is zero.

Now we can express the expectation value of  $X^2$  with only non-zero terms

$$\langle \hat{X}_{A_\sigma B_{\sigma'}}^{(\theta)^2} \rangle = \frac{1}{4} \left[ e^{-2i\phi} (\hat{a}_\sigma \hat{b}_{\sigma'} + \hat{b}_{\sigma'} \hat{a}_\sigma) + \hat{a}_\sigma^\dagger \hat{a}_\sigma + \hat{b}_{\sigma'}^\dagger \hat{b}_{\sigma'} \right] + h.c. \quad (11)$$

Let us first consider the expectation value of  $X^2$  for  $A_\uparrow$  and  $B_\uparrow$  modes. Substituting equation (10) in equation (9) we find

$$\langle \hat{X}_{\pm, A_\uparrow B_\uparrow}^{(\theta)^2} \rangle = \frac{1}{2} \left[ Re[S_{11} S_{13} e^{2i\phi}] + |S_{11}|^2 + |S_{13}|^2 + |S_{14}|^2 \right], \quad (12)$$

where

$$-2|S_{11}||S_{13}| \leq Re[S_{11} S_{13} e^{2i\phi}] \leq 2|S_{11}||S_{13}|.$$

We can obtain the maximum and the minimum value of  $\langle \hat{X}_{\pm, A_\uparrow B_\uparrow}^{(\theta)^2} \rangle$ , which are given by

$$\langle \hat{X}_{\pm, A_\uparrow B_\uparrow}^{(\theta)^2} \rangle = \frac{(\tilde{n}_\gamma - 1)}{2} + \frac{1}{2} |(\tilde{n}_g \tilde{n}_\gamma)^{1/2} \pm ((\tilde{n}_g - 1) \tilde{n}_\gamma)^{1/2}|^2, \quad (13)$$

and we obtain our equation (20) from the main text. For  $\gamma = 0$  we recover the two-mode squeezing in the spin-independent atomic dissociation in Ref. [4].

Similarly we can obtain equation (21) in our main text by switching  $S_{13}$  and  $S_{14}$  in equation (12).

- 
- [1] "Higher transcendental functions, edited by a. erdelyi, vol. 2 (mcgraw-hill, new york, 1953)."  
[2] Rajesh K. Malla, E. G. Mishchenko, and M. E. Raikh, "Suppression of the landau-zener transition probability by weak classical noise," *Phys. Rev. B* **96**, 075419 (2017).  
[3] N. A. Sinitsyn, "Solvable four-state landau-zener model of two interacting qubits with path interference," *Phys. Rev. B* **92**, 205431 (2015).  
[4] V. A. Yurovsky, A. Ben-Reuven, and P. S. Julienne, "Quantum effects on curve crossing in a Bose-Einstein condensate," *Phys. Rev. A* **65**, 043607 (2002).